Insulin gene enhancer binding protein 1 induces adipose tissue-derived stem cells to differentiate into pacemaker-like cells

JIAN ZHANG[1-3], MEI YANG[1-3], AN-KANG YANG[1-3], XI WANG[1-3], YAN-HONG TANG[1-3], QING-YAN ZHAO[1-3], TENG WANG[1-3], YU-TING CHEN[1-3] and CONG-XIN HUANG[1-3]

[1]Department of Cardiology, Renmin Hospital of Wuhan University; [2]Cardiovascular Research Institute, Wuhan University; [3]Hubei Key Laboratory of Cardiology, Wuhan, Hubei 430060, P.R. China

Received May 2, 2018; Accepted November 20, 2018

DOI: 10.3892/ijmm.2018.4002

Abstract. Hybrid approaches combining gene- and cell-based therapies to make biological pacemakers are a promising therapeutic avenue for bradyarrhythmia. The present study aimed to direct adipose tissue-derived stem cells (ADSCs) to differentiate specifically into cardiac pacemaker cells by overexpressing a single transcription factor, insulin gene enhancer binding protein 1 (ISL-1). In the present study, the ADSCs were transfected with ISL-1 or mCherry fluorescent protein lentiviral vectors and co-cultured with neonatal rat ventricular cardiomyocytes (NRVMs) *in vitro* for 5-7 days. The feasibility of regulating the differentiation of ADSCs into pacemaker-like cells by overexpressing ISL-1 was evaluated by observation of cell morphology and beating rate, reverse transcription-quantitative polymerase chain reaction analysis, western blotting, immunofluorescence and analysis of electrophysiological activity. In conclusion, these data indicated that the overexpression of ISL-1 in ADSCs may enhance the pacemaker phenotype and automaticity *in vitro*, features which were significantly increased following co-culture induction.

Introduction

Bradyarrhythmia, including bradycardia, sick sinus syndrome and atrioventricular block, is a group of diseases characterized by cardiac pacing or conduction dysfunction. Although drug therapy and electronic pacemakers have saved the lives of many patients with bradyarrhythmia, long-term medication cannot solve the underlying problem and there may be serious side effects, including wire break, electromagnetic interference, pocket infection, limited battery life and the lack of an independent reaction. With the progress of genetic engineering and molecular biology, biological pacemakers have emerged (1-3). Studies investigating biological pacemakers have primarily focused on the following two aspects: The restoration of cardiac pacing and conduction function. Studies have been performed to introduce specific genes into tissues with damaged autonomic rhythms or a damaged conduction system (4-9), in addition to transplanting pacemaker cells or pacemaker-like cells to repair or replace the damaged tissues (10-12).

To avoid problems with aberration and ethics, numerous studies have attempted to initiate automaticity in the atria and ventricles by using gene- and cell-based hybrid approaches (13-15). Stem cells have the potential for proliferation and pluripotent differentiation, and thus stem cell-derived pacemaker cells are the most common cell source. Adipose tissue-derived stem cells (ADSCs) are promising candidate cells for biological pacemakers, the advantages of which include accessibility, high harvesting efficiency and myocardial differentiation potential (16,17).

Insulin gene enhancer binding protein-1 (ISL-1), a subtype of the LIM homologous domain transcription factors, marks undifferentiated cardiac progenitor cells in the second heart field and is important in promoting cardiac development and differentiation (18,19). ISL-1-positive progenitor cells are able to differentiate into a variety of cell types in the heart and have persistent expression from the embryonic stage to adulthood in the murine sinoatrial node (SAN), compared with the transient expression of other components in the second heart field, which is consistent with results observed in the human SAN (20). At 9.5 embryonic days, ISL-1^{+} progenitor cells are primarily expressed in the venous sinus, namely the primitive pacemaker region, in early embryonic development (21). Sun *et al* (22) reported that ISL-1 is a specific marker for a subset of pacemaker cells at the developmental stages examined. ISL-1-expressing cells, organized as a ring-shaped structure around the venous pole, exhibit pacemaker functions and are able to rescue short stature homeobox 2-mediated bradycardia in the adult zebrafish heart (23,24). Vedantham *et al* (25) used RNA sequencing to confirm that ISL-1 has an upstream regulatory role in the development of bradycardia in the mouse SAN. Dorn *et al* (26) also confirmed that the overexpression of ISL-1 in embryonic stem cells or *Xenopus* embryos can lead to the upregulation of SAN-specific genes and the downregulation

Correspondence to: Professor Cong-Xin Huang, Department of Cardiology, Renmin Hospital of Wuhan University, 238 Jiefang Road, Wuchang, Wuhan, Hubei 430060, P.R. China
E-mail: huangcongxin@vip.163.com

Key words: bradyarrhythmia, insulin gene enhancer binding protein 1, adipose tissue-derived stem cells, biological pacing

of working myocardial genes. Liang *et al* (27) reported that ISL-1 is a necessary condition for development of the SAN, and influences the survival, reproduction and function of pacemaker cells.

Therefore, numerous studies have demonstrated that ISL-1 is located upstream of a variety of transcription factors and ion channels, and regulates the expression of SAN-specific genes. The present study examined whether ISL-1 was able to successfully direct the differentiation of ADSCs into pacemaker cells in order to provide a novel breakthrough for building an extracorporeal biological pacemaker by combining gene therapy with cell therapy.

Materials and methods

Animals. Adult male Sprague-Dawley (SD) rats (n=6; age, 3-4 weeks; weight, 40-80 g) and newborn SD rats (n=60; age, 1-3 days; weight, 5-10 g) were purchased from the Center for Disease Control and Prevention of Hubei Province (Hubei, China). All animals were housed in micro-isolators under specific pathogen-free conditions at 24˚C in a 12 h light/dark cycle, with free access to food and water. Animals received care in accordance with the guidelines for animal care published by the United States National Institutes of Health (Guide for the Care and Use of Laboratory Animals, Department of Health and Human Services, NIH Publication no. 86-23, revised 1985). The present study was approved by the Experimental Animal Committee of Wuhan University (Hubei, China; no. WDRM20171015).

Isolation and culture of ADSCs. All experimental procedures were conducted in accordance with the Institutional Guidelines for the Care and Use of Laboratory Animals at Wuhan University and conformed to the National Institutes of Health Guide for the Care and Use of Laboratory Animals. The adult male SD rats were anesthetized with an intraperitoneal injection of 2% pentobarbital sodium (40 mg/kg) and then sacrificed by cervical dislocation. ADSCs were obtained using a previously described method with modifications (28). Briefly, SD rat inguinal adipose tissue was digested in 5 ml Dulbecco's modified Eagle's medium (DMEM)/F-12 medium (cat. no. SH30023, HyClone; GE Healthcare Life Sciences, Logan, UT, USA) containing 0.1% (w/v) collagenase type I (cat. no. C0130, Sigma; Merck KGaA) at 37˚C for 45 min with gentle agitation. Following filtering and centrifugation at 1,000 x g for 10 min at room temperature, the floating top layer was discarded. The pellet was both washed and resuspended in DMEM/F-12 supplemented with 10% fetal bovine serum (FBS; cat. no. 16000-044; Gibco; Thermo Fisher Scientific, Inc., Waltham, MA, USA) and 1% penicillin/streptomycin (cat. no. 15070063, Invitrogen; Thermo Fisher Scientific, Inc.). The cells were seeded in 6-well plates (Corning, Inc., Corning, NY, USA) and incubated at 37˚C with a 5% CO_2 atmosphere. The medium was replaced every 2 days. When the cells reached 80-90% confluence, they were passaged using 0.25% trypsin (cat. no. GNM25200; Genom, Hangzhou, China). Cells at passages 3-5 were used for all subsequent experiments.

Construction of the human ISL-1 lentiviral vector and ISL-1 infection. The lentiviral vector expressing ISL-1 (Ubi-MCS-ISL-1-3FLAG-SV40-mCherry) was constructed by inserting the human ISL-1 gene (positive clone sequence: ATGGGAGACATGGGCGATCCACCAAAAAAAAAACGT CTGATTTCCCTGTGTGTTGGTTGCGGCAATCAAATT CACGACCAGTATATTCTGAGGGTTTCTCCGGATTTG GAGTGGCATGCAGCATGTTTGAAATGTGCGGAGTGT AATCAGTATTTGGACGAAAGCTGTACGTGCTTTGTT AGGGATGGGAAAACCTACTGTAAAAGAGATTATATC AGGTTGTACGGGATCAAATGCGCCAAGTGCAGCATA GGCTTCAGCAAGAACGACTTCGTGATGCGCGCCCGC TCTAAGGTGTACCACATCGAGTGTTTCCGCTGTGTA GCCTGCAGCCGACAGCTCATCCCGGGAGACGAATTC GCCCTGCGGGAGGATGGGCTTTTCTGCCGTGCAGAC CACGATGTGGTGGAGAGAGCCAGCCTGGGAGCTGGA GACCCTCTCAGTCCCTTGCATCCAGCGCGGCCTCTG CAAATGGCAGCCGAACCCATCTCGGCTAGGCAGCCA GCTCTGCGGCCGCACGTCCACAAGCAGCCGGAGAAG ACCACCCGAGTGCGGACTGTGCTCAACGAGAAGCAG CTGCACACCTTGCGGACCTGCTATGCCGCCAACCCT CGGCCAGATGCGCTCATGAAGGAGCAACTAGTGGAG ATGACGGGCCTCAGTCCCAGAGTCATCCGAGTGTGG TTTCAAAACAAGCGGTGCAAGGACAAGAAACGCAGC ATCATGATGAAGCAGCTCCAGCAGCAGCAACCCAAC GACAAAACTAATATCCAGGGGATGACAGGAACTCCC ATGGTGGCTGCTAGTCCGGAGAGACATGATGGTGGT TTACAGGCTAACCCAGTAGAGGTGCAAAGTTACCAG CCGCCCTGGAAAGTACTGAGTGACTTCGCCTTGCAA AGCGACATAGATCAGCCTGCTTTTCAGCAACTGGTC AATTTTTCAGAAGGAGGACCAGGCTCTAATTCTACT GGCAGTGAAGTAGCATCGATGTCCTCGCAGCTCCCA GATACACCCAACAGCATGGTAGCCAGTCCTATTGAG GCA) into the Ubi-MCS-3FLAG-SV40-Cherry vector (GeneChem Co., Ltd., Shanghai, China) using *Bam*HI (cat. no. FD0054) and *Age*I (cat. no. CON181) restriction sites, all obtained from GeneChem Co., Ltd. The ADSCs at passages 3-5 were removed from the culture dishes by digestion. A cell suspension was prepared and then inoculated onto 6-well plates. For infection, the cells were randomly divided into two groups: In group A, a lentivirus overexpressing mCherry or ISL-1-mCherry in DMEM/F-12 was added to the cells at different multiplicity of infection (MOI) values (MOI=0, 20, 50, 80 and 100) when cell confluence reached 30-50%; in group B, a lentivirus overexpressing mCherry or ISL-1-mCherry, 5-10 μg/ml polybrene (cat. no. H9268; Sigma; Merck KGaA) and enhanced infection solution (cat. no. REVG0002; GeneChem Co., Ltd.) were mixed together and added to the culture medium of cells at different MOI values (MOI=0, 20, 50, 80 and 100) when cell confluence reached 30-50%. The culture medium was replaced following culture at 37˚C in 5% CO_2 for 12-24 h, with the transfection time determined by the state of the cells.

Fluorescent microscope analysis and flow cytometric analysis. The expression of mCherry 48 h following infection of the cells was observed and recorded under a fluorescent microscope (BX51 system; Olympus Corporation, Tokyo, Japan). The transfected cells were digested with 0.25% trypsin at 72-96 h post-transfection and centrifuged at 1,000 x g for 5 min at room temperature. The cell density was 1-2x10^6/ml. Non-transfected cells served as a negative control. The percentage of red

Table I. Polymerase chain reaction primers used in the present study.

Gene		Primer sequence (5'-3')	Reaction conditions	Product size (bp)
H-ISL-1	Forward	5'-GGCAATCAAATTCACGACCA3'	50˚C 2 min, 95˚C 10 min; 95˚C	124
	Reverse	5'-CCCTAACAAAGCACGTACAGCT-3'	30 sec, 60˚C 30 sec, 40 cycles	
R-HCN4	Forward	5'-CACTAAGGGCAACAAGGAGACC-3'	50˚C 2 min, 95˚C 10 min; 95˚C	281
	Reverse	5'-GGTAGTTGAAGACGCCTGAGTTG-3'	30 sec, 60˚C 30 sec, 40 cycles	
R-Cx43	Forward	5'-GCTGGTGGTGTCCTTGGTGT-3'	50˚C 2 min, 95˚C 10 min; 95˚C	213
	Reverse	5'-GGAGGAGACATAGGCGAGAGTG-3'	30 sec, 60˚C 30 sec, 40 cycles	
R-Cx45	Forward	5'-CCCAGGCTATAACATTGCTGTC-3'	50˚C 2 min, 95˚C 10 min; 95˚C	198
	Reverse	5'-ATTGCTAGATCCAAGCGTTCC-3'	30 sec, 60˚C 30 sec, 40 cycles	
R-GAPDH	Forward	5'-CGCTAACATCAAATGGGGTG-3'	50˚C 2 min, 95˚C 10 min; 95˚C	201
	Reverse	5'-TTGCTGACAATCTTGAGGGAG-3'	30 sec, 60˚C 30 sec, 40 cycles	

ISL-1, insulin gene enhancer binding protein 1; Cx, connexin; GAPDH, glyceraldehyde 3-phosphate dehydrogenase.

fluorescent protein-positive cells was detected by flow cytometric analysis (BD Biosciences, Franklin Lakes, NJ, USA).

Isolation and culture of NRVMs and co-culture systems. Primary NRVMs were isolated from newborn SD rats in 1-3 days according to a previously described method with modifications (29). Briefly, the neonatal rat heart tissue was derived from newborn SD rats 1-3 days following sacrifice via cervical dislocation and was digested with 0.125% trypsin (cat. no. C0201, Beyotime Institute of Biotechnology, Shanghai, China) at 37˚C for 10 min. The precipitation were then repeatedly digested with mixed liquor containing 0.125% trypsin and 0.08% collagenase II (cat. no. C6885; Sigma; Merck KGaA) 5-8 times at 37˚C for 5 min. Following being filtered and centrifuged at 1,000 x g for 10 min at room temperature, the floating top layer was discarded. The pellets were resuspended and seeded in 6-well plates with fresh DMEM/F-12 supplemented with 15% FBS and 1% penicillin/streptomycin. The harvested NRVMs were purified by differential adhesion time to isolate the cardiomyocytes from the fibroblasts and 0.1 mmol/l bromodeoxyuridine (cat. no. B-5002, Sigma; Merck KGaA) to inhibit the mitosis of fibroblasts. For co-culture experiments, the ADSCs and NRVMs were mixed and plated at a ratio of 1:10 onto the 6-well plates (30,31). The complete culture medium was replaced every 2 days, and the cell morphology and beating rate were observed.

Reverse transcription-quantitative polymerase chain reaction (RT-qPCR) analysis. Total cellular RNA was extracted from the co-culture systems after 5-7 days using TRIzol reagent (cat. no. 15596-026, Invitrogen; Thermo Fisher Scientific, Inc.). The cDNA was produced using the PrimeScript™ RT reagent kit with gDNA Eraser (cat. no. RR047A, Takara Bio, Inc., Otsu, Japan) in a 15-μl mixture. All primers (Table I) for PCR amplification were synthesized by Invitrogen; Thermo Fisher Scientific, Inc. Reactions were carried out in a 20 μl reaction volume (containing 4 μl cDNA, 4 μl forward primer, 0.4 μl reverse primer, 10 μl SYBR Green Master mix, 0.4 μl 50X ROX reference dye 2 and 4.8 μl H_2O). RT-qPCR analysis was performed with standard SYBR® Premix Ex Taq™ (cat. no. RR420A, Takara Bio, Inc.) on a StepOne™ Real-Time PCR (Thermo Fisher Scientific, Inc.) instrument as follows: Pre-denaturation at 95˚C for 5 min, denaturation at 95˚C for 30 sec, annealing at 60˚C for 20 sec, and a final extension at 60˚C, a total of 40 cycles. The dissolution curve was from 60-95˚C and the temperature was raised by 1˚C per 20 sec. Relative gene expression was calculated using the $2^{-\Delta\Delta Cq}$ method (32) following normalization to glyceraldehyde 3-phosphate dehydrogenase (GAPDH) expression. To ensure accuracy, all results were repeated at least three times.

Western blot analysis. The cells were harvested using RIPA lysis buffer (cat. no. AS1004, Aspen Biological, Wuhan, China). Then the total protein concentrations in the sample were measured with a bicinchoninic acid kit (cat. no. AS1086; Aspen Biological) according to the manufacturer's protocol. The protein samples (40 μg protein each well) were mixed with 5X SDS-PAGE buffer (cat. no. AS1012; Aspen Biological) in a water bath at 95-100˚C for 5 min and transferred onto a polyvinylidene fluoride membranes. The membranes were incubated with primary antibodies against hyperpolarization-activated cyclic nucleotide-gated cation channel (HCN)4 (cat. no. ab32675), connexin (Cx)43 (cat. no. ab11370; both Abcam, Cambridge, MA, USA) and Cx45 (cat. no. F5108; Affinity Biosciences. OH, USA) overnight at 4˚C. Following at least three washes in Tris-buffered saline with Tween-20, the membranes were incubated for 30 min at room temperature with corresponding secondary antibodies: HRP-goat anti rat, (cat. no. AS1093) or HRP-goat anti rabbit (cat. no. AS1107; Aspen Biological), raised in the appropriate species. Specific bands of target proteins were then visualized using an enhanced chemiluminescence detection kit (cat. no. AS1059; Aspen Biological) according to the manufacturer's recommendations. The level of GAPDH was used to normalize the signal intensities. The image collection and densitometry analyses were performed with the Quantity One analysis software version 4.0 (AlphaEaseFC, Protein Simple, San Jose, CA, USA). The experiments were performed at least three times to verify results.

Immunofluorescence. The cell cultures were washed three times with phosphate-buffered saline (PBS; cat. no. GNB20012; Genom) and fixed with 4% paraformaldehyde (cat. no. AS1018; Aspen Biological) for 15 min at room temperature. Following washing in PBS, the cell were treated with 0.2% Triton (cat. no. T8787; Sigma; Merck KGaA) for 15 min. The cells then were incubated with the primary antibody anti-cardiac troponin T (cTnT, cat. no. ab19615, Abcam) or HCN4 (cat. no. ab8295; Abcam) overnight at 4˚C and incubated with goat anti-mouse or goat anti-rat secondary antibody Alexa Fluor 647 (cat. no. A0473; Beyotime Institute of biotechnology) or Alexa Fluor 647 (cat. no. ab150167; Abcam) for 50 min at room temperature. Nuclei stained with 4',6-diamidino-2-phenylindole was used as a location control. The fluorescent images were obtained with a Leica-LCS-SP8-STED confocal laser-scanning microscope (Leica Microsystems GmbH, Solms, Germany). Images were captured randomly of three visual fields in three samples to observe the positive rates of cTnT and HCN4 detection.

Electrophysiological recordings. Single, funny current (I_f) measurements were obtained by using a standard microelectrode whole-cell, patch-clamp technique with an Axon patch-clamp amplifier 700B (Molecular Devices LLC, Sunnyvale, CA, USA). A digital 700AD/DA converter and 6.0.4 pClamp (both Axon Instruments, Union City, CA, USA) were used for recording and analyzing the data. Following co-culture for 5-7 days, the cells were incubated with 180 μmol/l 2-aminoethoxydiphenyl borate (cat. no. D9754; Sigma; Merck KGaA) for 15 min to block intercellular electrical conduction. The cells were perfused with a normal Tyrode's solution containing (mmol/l): NaCl 135, KCl 5.4, $CaCl_2$ 1.8, $MgCl_2$ 1.0, glucose 10, $Bacl_2$ 2.0 and HEPES 5.5 (pH 7.4) with NaOH. Pipette solution contained (mmol/L): KCl 120, $Cacl_2$ 5.0, $MgCl_2$ 5.0, HEPES 10 and EGTA 10 (pH 7.3) with KOH. The impedance of the fluid filled electrode was 3-4 MΩ. The Clampex program was applied to the sample. The sampling frequency was 10 kHz, and the filtering rate was 5 kHz. The holding potential was set at -30mV, and a family of voltage steps from -140 to -40 mV for 1.5 sec with 20 mV increments was applied to elicit I_f. CsCl (4 mmol/l) was administered to detect the change in I_f.

Statistical analysis. All data are represented as the mean ± standard error of the mean. The statistical significance of the differences between two groups were analyzed using Student's t-test and comparisons among multiple groups were analyzed by one-way analysis of variance with SPSS 19.0 software (IBM Corp., Armonk, NY, USA). $P<0.05$ was considered to indicate a statistically significant difference.

Results

Culture of ADSCs and optimum MOI value for transfection. When initially isolated, the ADSCs appeared primarily round in shape. The ADSCs began to adhere at 4-5 h; a small number of cells became adherent with an irregular shape at 24 h; the largest number of cells became adherent and spindle-shaped with a relatively flat morphology, among which were cells with a high oval individual visible refractive index, at 48 h. Following culture for 5-7 days, the cell density reached ~90%. The sizes of the cultured cells were marginally different, based on their spindle-like morphology. The adjacent cells grew in a certain direction. As the number of passages increased, the sub-cultured cells were increasingly purified, homogenous and spindle-like. The cells reached 80-90% confluency in a fascicular-like or whirlpool-like manner following culture for 2-3 days (Fig. 1A). The rate of proliferation was significantly increased following propagation in culture. Sub-cultured cells at passage 3-5 were used in the present study.

At 2 days post-transfection, the red fluorescence of the infected ADSCs was detected by fluorescence microscopy in at least five randomly selected fields. The transfection efficiency was >80% at an MOI value of ≥50. At an MOI value of 80, certain fluorescent cells appeared as roundish cells with vacuoles in the cytoplasm, and gradually began to float. This phenomenon was more marked at an MOI of 100. Compared with group A, group B exhibited higher fluorescence intensity and clearer cell morphological features (Fig. 1B). The flow cytometric analysis demonstrated that the transfection efficiency of the ADSCs in group B reached 84.7±2.3% at an MOI value of 50 (Fig. 1C). With the increase in MOI, the fluorescence intensity and cell toxicity increased gradually (Fig. 1D). Through fluorescence microscopy and flow cytometric analyses, it was ascertained that the optimum MOI value for transfection was 50 using the transfection protocol of group B, and this was adopted for the following experiments. The mRNA expression of ISL-1 in the ISL-1-ADSCs group was significantly higher compared with that in the control group at day 5 post-transfection (Fig. 1E). The results demonstrated that ISL-1 achieved steady overexpression in the ADSCs.

Cell morphology and beating rate. The proliferation rate decreased and the morphology diversified following transfection, with the morphology dominated by the long spindle shape, in the ISL-1-ADSCs group compared with the mCherry-ADSCs group. Following co-culture for 2 days, the ADSCs and NRVMs had begun to form connections and cell clusters; the majority of cells were connected in a network and exhibited synchronous pulsation within a cluster following co-culture for 5 days; all cells had formed mutual a connection with a low but stable pulsation frequency following co-culture for 7 days (Fig. 2A). The morphology of the ADSCs was more irregular following co-culture with NRVMs, as determined by fluorescence microscopy, with three principal forms: Fusiform, triangular and quadrilateral (Fig. 2B).

The cells of the ISL-1-ADSCs group and mCherry-ADSCs group were not observed to be beating cells. Following co-culture with NRVMs, red-fluorescing ISL-1-transfected ADSCs were clearly observed to be spontaneously beating; however, red-fluorescing mCherry-transfected ADSCs were not spontaneously beating, although they exhibited synchronous pulsation driven by the surrounding cardiomyocytes, as determined by fluorescence microscopy. Furthermore, ADSCs transfected with ISL-1 had a higher pulsation frequency compared with the ADSCs transfected with mCherry and the NRVMs without ADSCs. The beating rate of the cells reached ~92±6.42 bpm (n=15) in the ISL-1-ADSCs+NRVM group at day 5. By comparison, the beating rate of the cells in the mCherry-ADSCs+NRVM group was ~73.67±7.09 bpm (n=15)

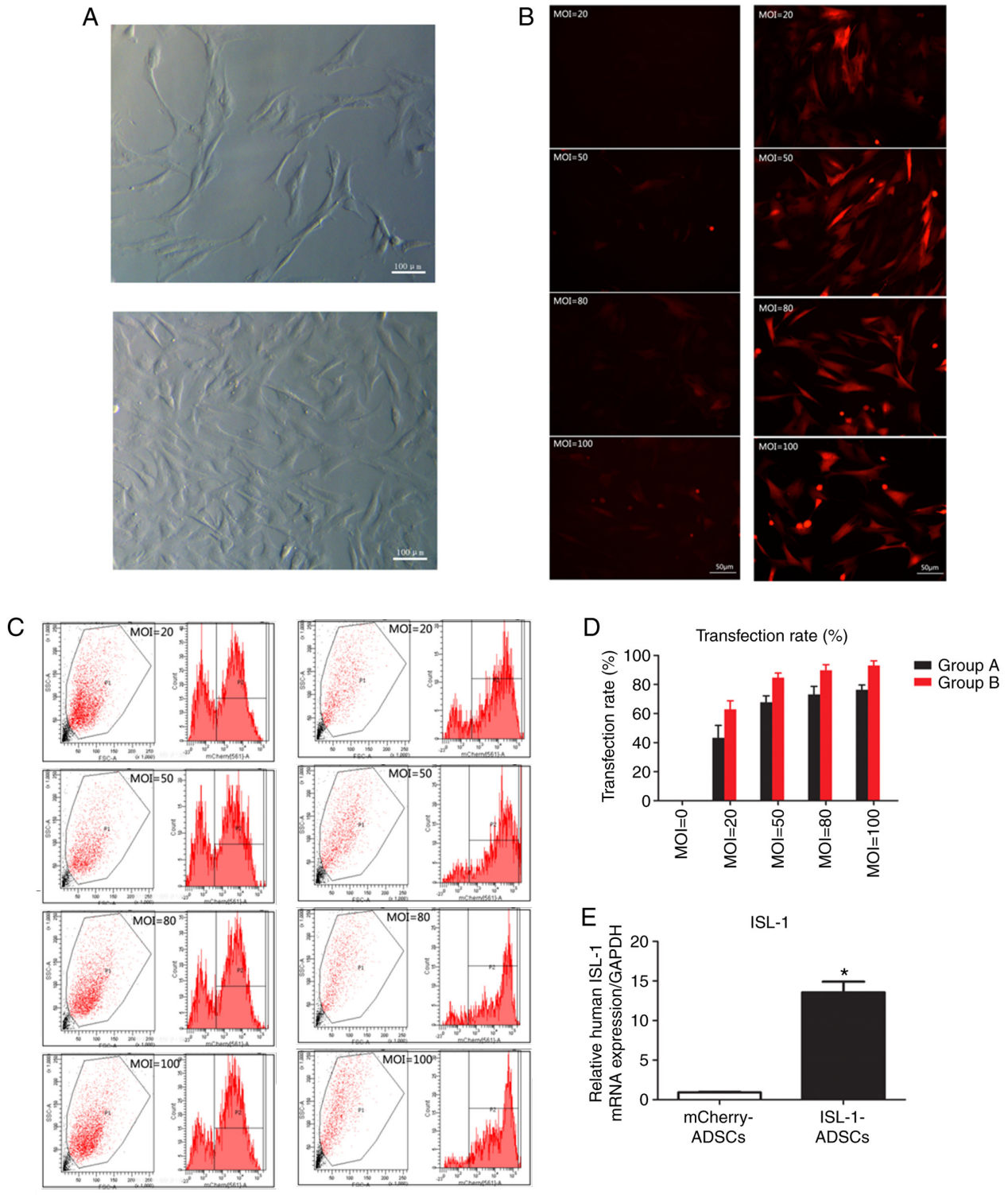

Figure 1. Transfection rate and the expression of ISL-1. (A) ADSCs observed following culture for 48 h and 5-7 days under a light microscope (magnification, x100). (B) ISL-1-ADSCs observed under a fluorescence microscope at different MOI values (magnification, x200). (C) Numbers of positive cells at MOI values detected by flow cytometric analysis. (D) Transfection rate at different MOI values. In group A, cells were transfected with lentivirus overexpressing mCherry or ISL-1-mCherry. In group B, cells were transfected with a mix of lentivirus overexpressing mCherry or ISL-1-mCherry, 5-10 μg/ml polybrene and enhanced infection solution. (E) mRNA expression of human ISL-1 in the transfected groups. *P<0.05, vs. mCherry-ADSCs. ADSCs, adipose tissue-derived stem cells; ISL-1, insulin gene enhancer binding protein 1; GAPDH, glyceraldehyde 3-phosphate dehydrogenase; MOI, multiplicity of infection.

at day 5; the beating rate of the NRVMs without ADSCs was ~80.17±8.13 bpm (n=15) at day 5 (Fig. 2C).

Expression of associated proteins and genes assessed by western blotting and RT-qPCR. To evaluate the role of ISL-1 in the differentiation of the SAN, the expression status of a number of genes that are known to be important for SAN formation and function was investigated. The genes detected in the present study included: HCN4, a crucial marker of pacemaker cells; Cx45, which prevents the formation of areas

of conductivity inside the SAN; and Cx43, a marker of the working myocardium. As presented in Fig. 3A-C, the mRNA and protein expression levels of HCN4 and Cx45 were significantly increased in the ADSCs transfected with ISL-1 lentivirus (ISL-1-ADSCs group) compared with the empty lentivirus group (mCherry-ADSCs group), and the difference was statistically increased when co-cultured with NRVMs ($P<0.05$). By contrast, the mRNA and protein expression levels of CX43 were significantly increased in the group co-cultured with NRVMs, and downregulated in the ISL-1-ADSCs+NRVMs group compared with the mCherry-ADSCs+NRVMs group ($P<0.05$).

Localization of associated gene expression in co-culture systems, as assessed by immunofluorescence. As demonstrated in Fig. 4, cTnT, a myocardium-specific marker, and HCN4, a marker of SAN function, were detected by immunofluorescence following co-culture for 5-7 days. The ADSCs were randomly distributed in the culture and a large number existed in a plane below the NRVMs, with some interspersed between the NRVMs. The immunofluorescence staining results revealed that the NRVMs and cardiac muscle-like cells were all positive for the expression of cTnT, and that the ADSCs transfected with ISL-1 had abundant positive staining for HCN4 protein. However, in the mCherry-transfected group, cTnT and HCN4 protein expression was barely detectable. The ADSCs transfected with ISL-1 also exhibited a high percentage of cells positive for the specific proteins, compared with negative control cells.

Electrophysiological recording in pacemaker-like cells. The red fluorescent cells were used for detecting intracellular electrical activity via the patch clamp method (Fig. 5A). The I_f, a key contributor to spontaneous phase four depolarization, was significantly detected in the transfected-ISL-1-ADSCs and ISL-1-ADSCs+NRVMs, although not in the control group or NRVMs. Following co-culture with NRVMs, transfected-ISL-1-ADSCs recorded a greater inward current. The ISL-1-ADSCs had an inward current (~1/20 cells) that was activated by the hyperpolarization intervals from -40 mV. The current had clear dependent characteristics of time and voltage and was sensitive to CsCl. The current was completely inhibited following the addition of CsCl blocker (4 mmol/l) to the extracellular fluid (Fig. 5B). When CsCl was eluted from the extracellular fluid, the inward current resumed rapidly. With the increase in density-voltage and time, the inward current gradually increased (Fig. 5C). Therefore, the current was markedly voltage- and time-dependent.

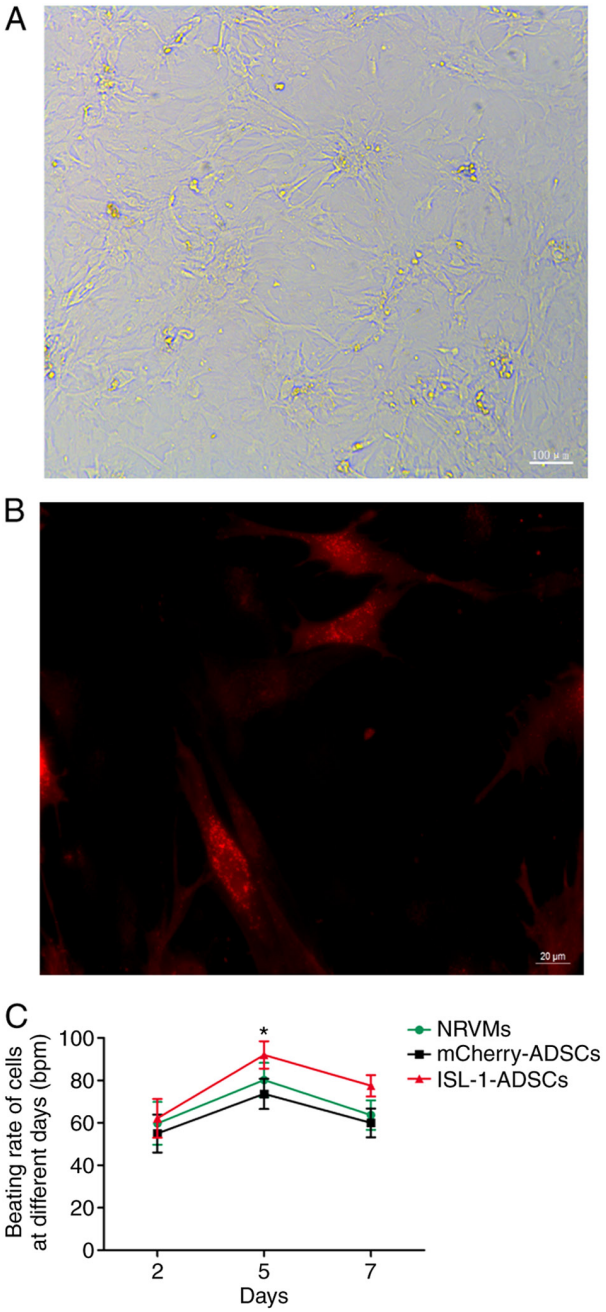

Figure 2. Cell morphology and beating rate in co-culture systems. (A) Morphology of ADSCs following co-culture under a light microscope (magnification, x100). (B) Morphology of ADSCs following co-culture under a fluorescence microscope (magnification, x400). (C) Beating rate of ADSCs and NRVMs on different days in the co-culture system. Green represents NRVMs on different days in the NRVMs only group; black represents the beating rate of mCherry-ADSCs in the co-culture system; red represents the beating rate of ISL-1-ADSCs in the co-culture system, $^*P<0.05$. ADSCs, adipose tissue-derived stem cells; NRVMs, neonatal rat ventricular cardiomyocytes; ISL-1, insulin gene enhancer binding protein 1.

Discussion

It is well known that ISL-1 is essential to the proper formation and development of the heart. ISL1-positive cells, isolated from embryonic stem cells (ESCs), induced pluripotent stem cells, bone mesenchymal stem cells and embryonic or postnatal heart tissues, have the potential to give rise to diverse cell types in the cardiovascular system, including cardiomyocytes, smooth muscle cells, endothelial cells and pacemaker cells (33-35). ISL-1-overexpressing cardiomyocytes exhibit higher beating frequencies in mouse ESC-derived regions and *Xenopus* hearts, which are associated with the upregulation of nodal-specific genes and the downregulation of genes associated with the working myocardium (26). However, ADSCs have high harvesting efficiency and pluripotency potential and, for these reasons, offer promise for biological pacing therapy in the future. At present, to the best of our knowledge, no investigations of biological pacemakers have provided direct evidence as to whether or not ADSCs may

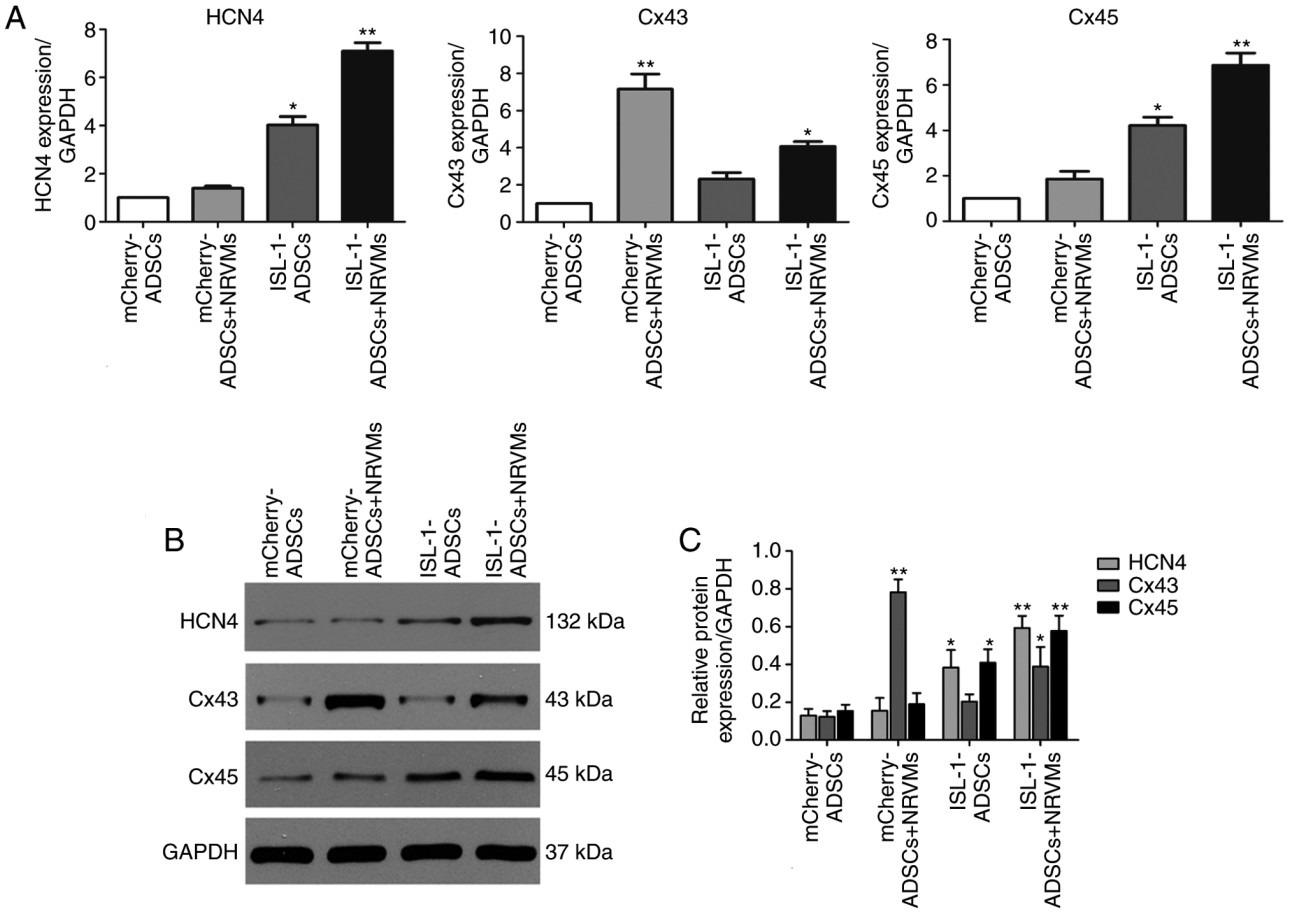

Figure 3. Expression of related genes by western blot and RT-qPCR analyses following co-culture for 5-7 days. (A) Gene expression levels of HCN4, Cx45 and Cx43 were examined by RT-qPCR analysis. (B) Protein expression of HCN4, Cx45 and Cx43 was examined using western blotting. (C) Quantitative assessment of protein levels of HCN4, Cx45 and Cx43 by integrated optical density analyses. Similar results were obtained in three independent experiments. GAPDH was used as the protein control. *P<0.05 vs. other groups, **P<0.01, vs. other groups. HCN4, hyperpolarization-activated cyclic nucleotide-gated cation channel 4; Cx45, connexin 45; Cx43, connexin 43; GAPDH, glyceraldehyde 3-phosphate dehydrogenase; ADSCs, adipose tissue-derived stem cells; NRVMs, neonatal rat ventricular cardiomyocytes; ISL-1, insulin gene enhancer binding protein 1; RT-qPCR, reverse transcription-quantitative polymerase chain reaction.

be induced to become pacemaker cells via the single ISL-1 transcription factor. Therefore, it is particularly important to examine the role of the single ISL-1 transcription factor in building a biological pacemaker. In the present study, ISL-1 was overexpressed via lentiviral vectors to identify whether a single transcription factor may be sufficient to induce the differentiation of ADSCs into pacemaker-like cells. To identify whether the cells transfected with ISL-1 had the specific phenotypes and functions of pacemaker-like cells, the outcomes were evaluated through morphological detection, RT-qPCR analysis, western blotting, immunofluorescence and electrophysiological monitoring.

There are a number of principal methods for inducing cardiomyocyte differentiation in stem cells, including biochemical induction, cardiac microenvironment induction and genetic modification (26). Co-culturing with NRVMs has been demonstrated to generate a model mimicking the physiological microenvironment of the heart following genetic modification by cellular factors, chemical substances, electrical activity and mechanical stretching (36). Studies have demonstrated that direct contact, rather than indirect contact, is more essential for adult stem cells to successfully differentiate into myocardial cells (30,31). Therefore, the transfected ADSCs were directly co-cultured with NRVMs at a 1:10 ratio, in order to induce differentiation of the stem cells in the present study. It was found that the morphology of the ADSCs altered following transfection with ISL-1 and was more irregular following co-culture with NRVMs. The expression of ISL-1 markedly increased the percentage of spontaneously beating ADSCs.

The above observation was accompanied by the altered expression of a number of genes essential for SAN formation. HCN channels are expressed throughout cardiac development (37). HCN4 exhibits the highest expression among the four HCN genes (HCN1-4) and is maintained until adulthood in the SAN (38). Studies on numerous species have demonstrated that HCN4 is key in the generation of the SAN, although a low level of HCN4 has be observed in human and mouse atrial and ventricular myocytes (39-42). Therefore, HCN4 may be considered a specific marker of the SAN region. In our previous study, it was demonstrated that the overexpression of ISL-1 in ADSCs was able to upregulate the expression level of HCN4 *in vitro,* and its level was significantly increased by co-culture induction. Four principal connexins have been identified to be expressed in different cardiac tissues, including Cx40, Cx30.2, Cx43 and Cx45 (43).

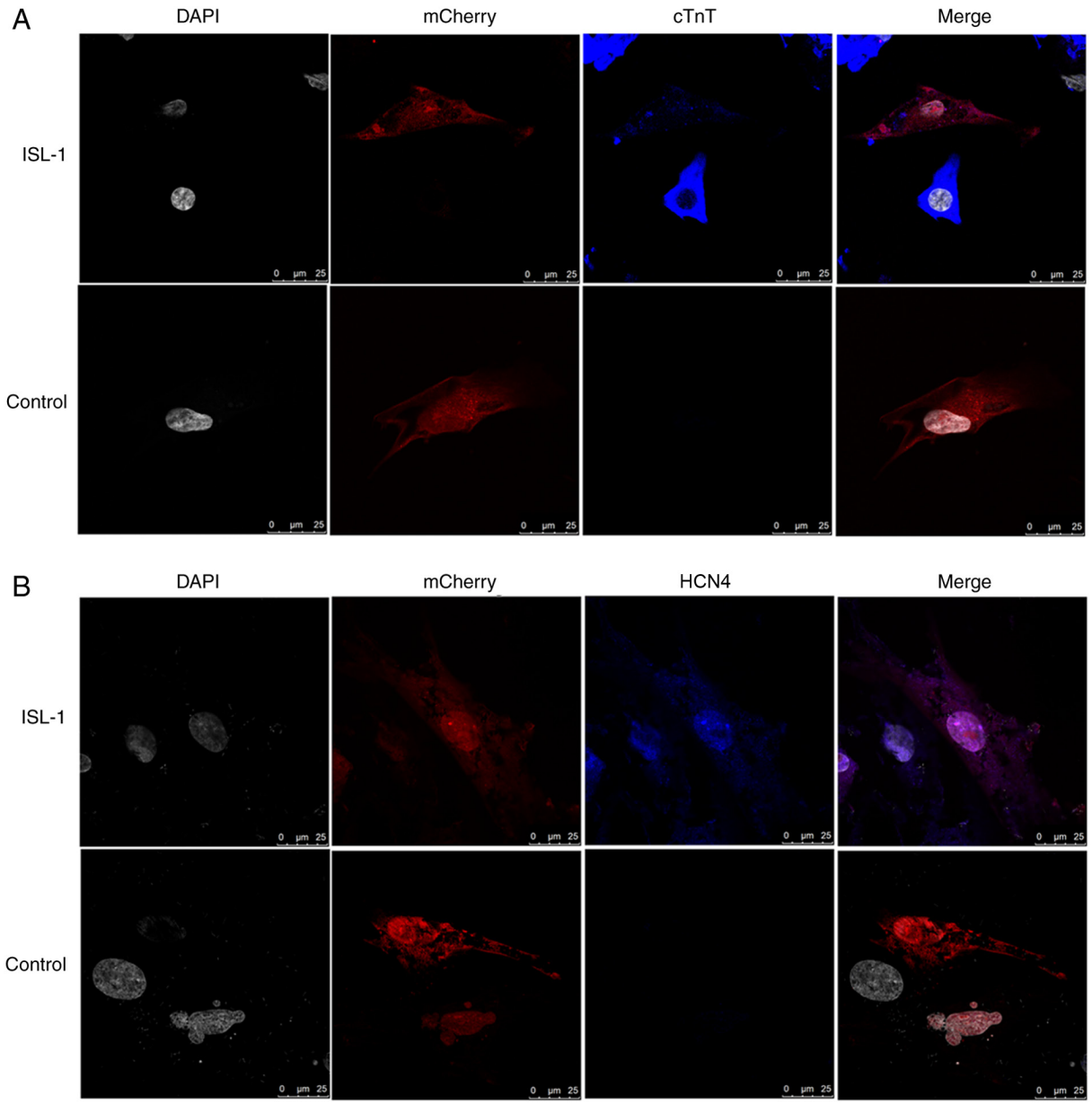

Figure 4. Cardiac-specific proteins examined by immunofluorescence staining in differentiated ADSCs following co-culture for 5-7 days with NRVMs (magnification, x400). (A) Clear positive staining for cTnT was observed in ADSCs transfected with Ubi-MCS-ISL-1-3FLAG-SV40-mCherry and Ubi-MCS-3FLAG-SV40-mCherry control vector. (B) Clear positive staining for HCN4 was observed in ADSCs transfected with Ubi-MCS-ISL-1-3FLAG -SV40-mCherry and Ubi-MCS-3FLAG-SV40-mCherry control vector. Scale bar, 25 μm. The nuclei were stained with DAPI (grey), mCherry-ADSCs were detected by immunofluorescence (red). Representative positive staining of HCN4 and cTnT is shown in blue. ADSCs, adipose tissue-derived stem cells; ISL-1, insulin gene enhancer binding protein 1; HCN4, hyperpolarization-activated cyclic nucleotide-gated cation channel; DAPI, 4',6-diamidino-2-phenylindole.

To prevent the SAN from over-suppressing the more hyperpolarized non-pacing atrial muscle surrounding the SAN, electrical coupling should be weak in the center of the SAN. Furthermore, to ensure that the SAN is able to drive the atrial muscle, electrical coupling must be strong in the periphery of the SAN. Consistent with this, Cx43 is the dominant connexin in working myocytes and Cx45 is primarily expressed in the center of the SAN, which directly connects nodal cells with atrial myocytes; cardiomyoblast cells express a combination of Cx43 and Cx45 in the periphery of the SAN (44,45). In the present study, Cx45 was also upregulated in ISL-1-transfected ADSCs, and the differences became more marked when the cells were co-cultured with NRVMs. Cx43 was downregulated in the ISL-1-transfected ADSCs but was upregulated following co-culture, possibly due to the addition of NRVMs. Therefore, it was suggested that ISL-1 may promote pacemaker differentiation by enhancing the expression of HCN4 and Cx45 *in vitro* and reducing the expression of Cx43 in the working myocardium.

Cardiac pacemaker activity originates from the SAN. The automaticity of the SAN is due to slow diastolic depolarization. There are two clocks that act interdependently and synergistically to initiate the heartbeat, modulated by autonomic neurons, including the voltage clock generated by HCN channels, referred to as I_f, the funny current; and the calcium clock generated by rhythmic Ca^{2+} release from the sarcoplasmic reticulum (46-48). In the present study, the typical I_f current demonstrated that the overexpression of

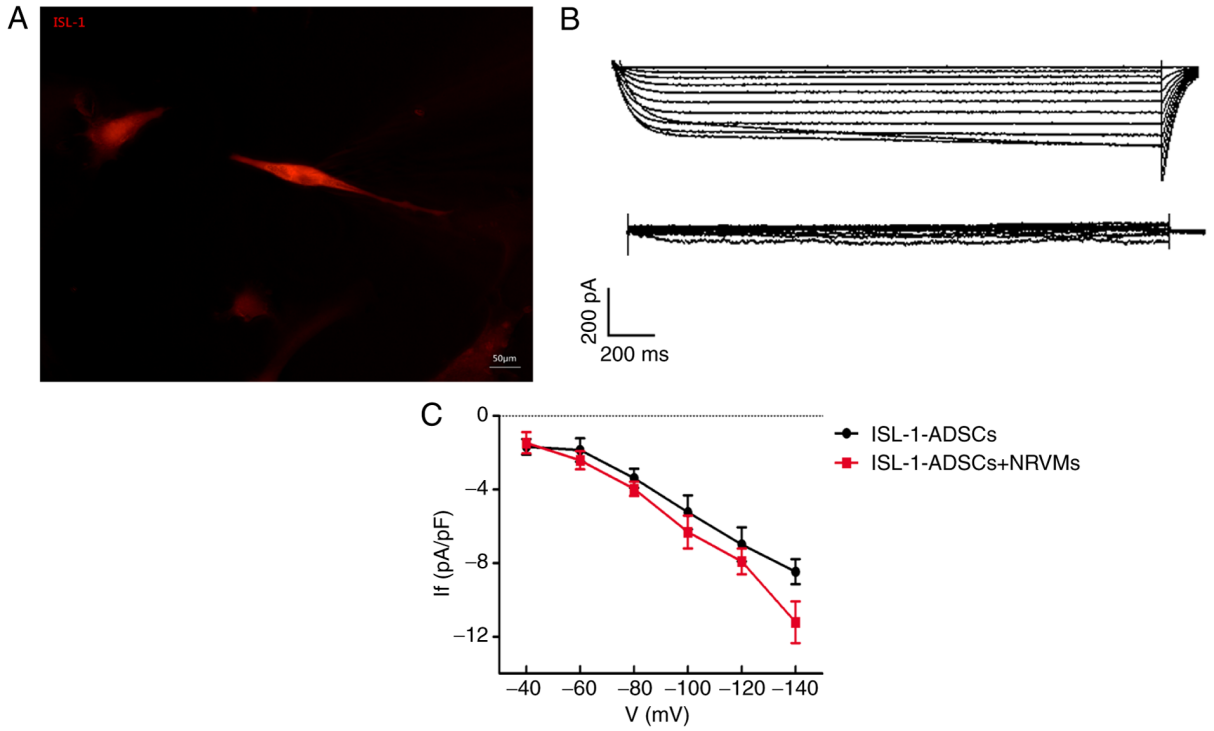

Figure 5. Spontaneous electrical activity in differentiated ADSCs. (A) Spindle-shaped cells were used for electrophysiological recordings (magnification, x200). (B) I_f current was detected in ISL-1-ADSCs using the patch clamp technique and was blocked by CsCl (4 mM/l). (C) Current density-voltage relationships of ISL-1-ADSCs (black, n=6) and ISL-1-ADSCs+NRVMs (red, n=6) groups. ADSCs, adipose tissue-derived stem cells; ISL-1, insulin gene enhancer binding protein 1; NRVMs, neonatal rat ventricular cardiomyocytes; I_f, hyperpolarization-activated inward current.

ISL-1 in ADSCs resulted in normal electrophysiologically functional cells, which were enriched in the nodal subtype at the expense of the ventricular lineage. Following initial heart tube formation, the heart tube elongates via the addition of ISL-1- and NK2 homeobox 5 (Nkx2.5)-positive progenitor cells, which maintain their expression until cardiac differentiation (21). The regulatory association between ISL-1 and Nkx2.5 may also exhibit opposite effects (26) Nkx2.5 is able to induce differentiation in the working myocardium, resulting in the downregulation of HCN4 and Tbx3, and the ectopic expression of Cx40 and natriuretic peptide A in the SAN region (49). By contrast, ISL-1 is able to upregulate nodal-specific genes and downregulate transcripts associated with the working myocardium to induce differentiation of the SAN. The results of the present study demonstrated that the morphology, biochemical characteristics and electrophysiological characteristics of ADSCs altered considerably following co-culture with NRVMs. This indicated that the cardiac microenvironment is important in inducing stem cells to differentiate into pacemaker-like cells. Furthermore, it suggested that the *in vivo* environment may improve the quality of pacemaker-like cells.

In conclusion, the present results suggested that ISL-1-transfected ADSCs had been successfully transformed into spontaneously beating cells that exhibited behaviors similar to those of pacemaker cells. The following lines of evidence support this result: i) The finding of transfected cells with morphological features distinctive to pacemaker-like cells; ii) characteristic mRNA and protein alterations, including the upregulation of HCN4 and Cx45, and the suppression of Cx43; iii) the localization of the expression of HCN4 and cTnT, as demonstrated by immunofluorescence; and iv) I_f, the current specific to the SAN, was recorded in ISL-1-transfected cells. However, the present study had a number of limitations. No further animal experiments were performed owing to the low efficiency of lentivirus transfection. In addition, the Na^+ ion currents, K^+ ion currents, and action potential of the cells was not examined due to technical and instrumental limitations. The present findings are not intended to be used as a direct precursor to the long-term application of biological pacing tools, as further investigation in *in vivo* animal models is required to evaluate safety and validity prior to application in patients with sinus dysfunction. However, the results of the present study may provide insights into the progression of pacemaker cell development, as these cells are reflected in the ADSC system, and this may offer a new perspective for the examination of a novel approach in the generation of biological pacemakers.

Acknowledgements

The authors are grateful to Wuhan University School of Basic Medical Science and the Medical Research Center for Structural Biology for their assistance in conducting the experiments on the fluorescent images.

Funding

The present study was supported by the Fundamental Research Funds for the Central Universities of China (grant no. 2042015kf0229).

Availability of data and materials

All data generated and analyzed during this study are included in this published article.

Authors' contributions

JZ made substantial contributions to the conception and design of the study, performed the experiments and wrote the paper. MY, AKY and YTC assisted in the development of experiments and analyzed the data. XW, YHT, QYZ and TW participated in research design and coordinated the study. CXH revised the manuscript and gave final approval of the version to be published. All authors read and approved the final manuscript.

Ethics approval and consent to participate

Ethics approval was provided by the Ethics Committee of Wuhan University.

Patient consent for publication

Not applicable.

Competing interests

The authors declare that they have no competing interests.

References

1. Cho HC and Marbán E: Biological therapies for cardiac arrhythmias: Can genes and cells replace drugs and devices? Circ Res 106: 674-685, 2010.
2. Boink GJ, Christoffels VM, Robinson RB and Tan HL: The past, present, and future of pacemaker therapies. Trends Cardiovasc Med 25: 661-673, 2015.
3. Cingolani E, Goldhaber JI and Marban E: Next-generation pacemakers: From small devices to biological pacemakers. Nat Rev Cardiol 15: 139-150, 2018.
4. Edelberg JM, Aird WC and Rosenberg RD: Enhancement of murine cardiac chronotropy by the molecular transfer of the human beta2 adrenergic receptor cDNA. J Clin Invest 101: 337-343, 1998.
5. Boink GJ, Nearing BD, Shlapakova IN, Duan L, Kryukova Y, Bobkov Y, Tan HL, Cohen IS, Danilo P Jr, Robinson RB, *et al*: Ca(2+)-stimulated adenylyl cyclase AC1 generates efficient biological pacing as single gene therapy and in combination with HCN2. Circulation 126: 528-536, 2012.
6. Miake J, Marbán E and Nuss HB: Biological pacemaker created by gene transfer. Nature 419: 132-133, 2002.
7. Qu J, Plotnikov AN, Danilo P Jr, Shlapakova I, Cohen IS, Robinson RB and Rosen MR: Expression and function of a biological pacemaker in canine heart. Circulation 107: 1106-1109, 2003.
8. Bucchi A, Plotnikov AN, Shlapakova I, Danilo P Jr, Kryukova Y, Qu J, Lu Z, Liu H, Pan Z, Potapova I, *et al*: Wild-type and mutant HCN channels in a tandem biological-electronic cardiac pacemaker. Circulation 114: 992-999, 2006.
9. Boink GJ, Duan L, Nearing BD, Shlapakova IN, Sosunov EA, Anyukhovsky EP, Bobkov E, Kryukova Y, Ozgen N, Danilo P Jr, *et al*: HCN2/SkM1 gene transfer into canine left bundle branch induces stable, autonomically responsive biological pacing at physiological heart rates. J Am Coll Cardiol 61: 1192-1201, 2013.
10. Ruhparwar A, Tebbenjohanns J, Niehaus M, Mengel M, Irtel T, Kofidis T, Pichlmaier AM and Haverich A: Transplanted fetal cardiomyocytes as cardiac pacemaker. Eur J Cardiothorac Surg 21: 853-857, 2002.
11. Kehat I, Khimovich L, Caspi O, Gepstein A, Shofti R, Arbel G, Huber I, Satin J, Itskovitz-Eldor J and Gepstein L: Electromechanical integration of cardiomyocytes derived from human embryonic stem cells. Nat Biotechnol 22: 1282-1289, 2004.
12. Xue T, Cho HC, Akar FG, Tsang SY, Jones SP, Marbán E, Tomaselli GF and Li RA: Functional integration of electrically active cardiac derivatives from genetically engineered human embryonic stem cells with quiescent recipient ventricular cardiomyocytes: Insights into the development of cell-based pacemakers. Circulation 111: 11-20, 2005.
13. Plotnikov AN, Shlapakova I, Szabolcs MJ, Danilo P Jr, Lorell BH, Potapova IA, Lu Z, Rosen AB, Mathias RT, Brink PR, *et al*: Xenografted adult human mesenchymal stem cells provide a platform for sustained biological pacemaker function in canine heart. Circulation 116: 706-713, 2007.
14. Shlapakova IN, Nearing BD, Lau DH, Boink GJ, Danilo P Jr, Kryukova Y, Robinson RB, Cohen IS, Rosen MR and Verrier RL: Biological pacemakers in canines exhibit positive chronotropic response to emotional arousal. Heart Rhythm 7: 1835-1840, 2010.
15. Chauveau S, Anyukhovsky EP, Ben-Ari M, Naor S, Jiang YP, Danilo P Jr, Rahim T, Burke S, Qiu X, Potapova IA, *et al*: Induced pluripotent stem cell-derived cardiomyocytes provide in vivo biological pacemaker function. Circ Arrhythm Electrophysiol 10: e004508, 2017.
16. Dmitrieva RI, Minullina IR, Bilibina AA, Tarasova OV, Anisimov SV and Zaritskey AY: Bone marrow- and subcutaneous adipose tissue-derived mesenchymal stem cells: Differences and similarities. Cell Cycle 11: 377-383, 2012.
17. Joo HJ, Kim JH and Hong SJ: Adipose tissue-derived stem cells for myocardial regeneration. Korean Circ J 47: 151-159, 2017.
18. Brade T, Gessert S, Kuhl M and Pandur P: The amphibian second heart field: *Xenopus* islet-1 is required for cardiovascular development. Dev Biol 311: 297-310, 2007.
19. Bu L, Jiang X, Martin-Puig S, Caron L, Zhu S, Shao Y, Roberts DJ, Huang PL, Domian IJ and Chien KR: Human ISL1 heart progenitors generate diverse multipotent cardiovascular cell lineages. Nature 460: 113-117, 2009.
20. Weinberger F, Mehrkens D, Friedrich FW, Stubbendorff M, Hua X, Müller JC, Schrepfer S, Evans SM, Carrier L and Eschenhagen T: Localization of Islet-1-positive cells in the healthy and infarcted adult murine heart. Circ Res 110: 1303-1310, 2012.
21. Mommersteeg MT, Dominguez JN, Wiese C, Norden J, de Gier-de VC, Burch JB, Kispert A, Brown NA, Moorman AF and Christoffels VM: The sinus venosus progenitors separate and diversify from the first and second heart fields early in development. Cardiovasc Res 87: 92-101, 2010.
22. Sun Y, Liang X, Najafi N, Cass M, Lin L, Cai CL, Chen J and Evans SM: Islet 1 is expressed in distinct cardiovascular lineages, including pacemaker and coronary vascular cells. Dev Biol 304: 286-296, 2007.
23. Tessadori F, van Weerd JH, Burkhard SB, Verkerk AO, de Pater E, Boukens BJ, Vink A, Christoffels VM and Bakkers J: Identification and functional characterization of cardiac pacemaker cells in zebrafish. PLoS One 7:e47644, 2012.
24. Hoffmann S, Berger IM, Glaser A, Bacon C, Li L, Gretz N, Steinbeisser H, Rottbauer W, Just S and Rappold G: Islet1 is a direct transcriptional target of the homeodomain transcription factor Shox2 and rescues the Shox2-mediated bradycardia. Basic Res Cardiol 108: 339, 2013.
25. Vedantham V, Galang G, Evangelista M, Deo RC and Srivastava D: RNA sequencing of mouse sinoatrial node reveals an upstream regulatory role for Islet-1 in cardiac pacemaker cells. Circ Res 116: 797-803, 2015.
26. Dorn T, Goedel A, Lam JT, Haas J, Tian Q, Herrmann F, Bundschu K, Dobreva G, Schiemann M, Dirschinger R, *et al*: Direct nkx2-5 transcriptional repression of isl1 controls cardiomyocyte subtype identity. Stem Cells 33: 1113-1129, 2015.
27. Liang X, Zhang Q, Cattaneo P, Zhuang S, Gong X, Spann NJ, Jiang C, Cao X, Zhao X, Zhang X, *et al*: Transcription factor ISL1 is essential for pacemaker development and function. J Clin Invest 125: 3256-3268, 2015.
28. Bunnell BA, Flaat M, Gagliardi C, Patel B and Ripoll C: Adipose-derived stem cells: Isolation, expansion and differentiation. Methods 45: 115-120, 2008.
29. Golden HB, Gollapudi D, Gerilechaogetu F, Li J, Cristales RJ, Peng X and Dostal DE: Isolation of cardiac myocytes and fibroblasts from neonatal rat pups. Methods Mol Biol 843: 205-214, 2012.

30. Zhu Y, Liu T, Song K, Ning R, Ma X and Cui Z: ADSCs differentiated into cardiomyocytes in cardiac microenvironment. Mol Cell Biochem 324: 117-129, 2009.
31. Choi YS, Dusting GJ, Stubbs S, Arunothayaraj S, Han XL, Collas P, Morrison WA and Dilley RJ: Differentiation of human adipose-derived stem cells into beating cardiomyocytes. J Cell Mol Med 14: 878-889, 2010.
32. Livak KJ and Schmittgen TD: Analysis of relative gene expression data using real-time quantitative PCR and the 2(-Delta Delta C(T)) method. Methods 25: 402-408, 2001.
33. Moretti A, Caron L, Nakano A, Lam JT, Bernshausen A, Chen Y, Qyang Y, Bu L, Sasaki M, Martin-Puig S, *et al*: Multipotent embryonic isl1+ progenitor cells lead to cardiac, smooth muscle, and endothelial cell diversification. Cell 127: 1151-1165, 2006.
34. Moretti A, Bellin M, Jung CB, Thies TM, Takashima Y, Bernshausen A, Schiemann M, Fischer S, Moosmang S, Smith AG, *et al*: Mouse and human induced pluripotent stem cells as a source for multipotent Isl1+ cardiovascular progenitors. FASEB J 24: 700-711, 2010.
35. Yi Q, Xu H, Yang K, Wang Y, Tan B, Tian J and Zhu J: Islet-1 induces the differentiation of mesenchymal stem cells into cardiomyocyte-like cells through the regulation of Gcn5 and DNMT-1. Mol Med Rep 15: 2511-2520, 2017.
36. Shen H, Wang Y, Zhang Z, Yang J, Hu S and Shen Z: Mesenchymal stem cells for cardiac regenerative therapy: Optimization of cell differentiation strategy. Stem Cells Int 2015: 524756, 2015.
37. Schuleri KH, Boyle AJ and Hare JM: Mesenchymal stem cells for cardiac regenerative therapy. Handb Exp Pharmacol: 195-218, 2007.
38. Biel M, Schneider A and Wahl C: Cardiac HCN channels: Structure, function, and modulation. Trends Cardiovasc Med 12: 206-212, 2002.
39. Shi W, Wymore R, Yu H, Wu J, Wymore RT, Pan Z, Robinson RB, Dixon JE, McKinnon D and Cohen IS: Distribution and prevalence of hyperpolarization-activated cation channel (HCN) mRNA expression in cardiac tissues. Circ Res 85: e1-e6, 1999.
40. Liu J, Dobrzynski H, Yanni J, Boyett MR and Lei M: Organisation of the mouse sinoatrial node: Structure and expression of HCN channels. Cardiovasc Res 73: 729-738, 2007.
41. Zicha S, Fernández-Velasco M, Lonardo G, L'Heureux N and Nattel S: Sinus node dysfunction and hyperpolarization-activated (HCN) channel subunit remodeling in a canine heart failure model. Cardiovasc Res 66: 472-481, 2005.
42. Li N, Csepe TA, Hansen BJ, Dobrzynski H, Higgins RS, Kilic A, Mohler PJ, Janssen PM, Rosen MR, Biesiadecki BJ and Fedorov VV: Molecular mapping of sinoatrial node HCN channel expression in the human heart. Circ Arrhythm Electrophysiol 8: 1219-1227, 2015.
43. Gros DB and Jongsma HJ: Connexins in mammalian heart function. Bioessays 18: 719-730, 1996.
44. Martinez AD, Hayrapetyan V, Moreno AP and Beyer EC: Connexin43 and connexin45 form heteromeric gap junction channels in which individual components determine permeability and regulation. Circ Res 90: 1100-1107, 2002.
45. Boyett MR, Inada S, Yoo S, Li J, Liu J, Tellez J, Greener ID, Honjo H, Billeter R, Lei M, *et al*: Connexins in the sinoatrial and atrioventricular nodes. Adv Cardiol 42: 175-197, 2006.
46. Lakatta EG, Vinogradova T, Lyashkov A, Sirenko S, Zhu W, Ruknudin A and Maltsev VA: The integration of spontaneous intracellular Ca2+ cycling and surface membrane ion channel activation entrains normal automaticity in cells of the heart's pacemaker. Ann NY Acad Sci 1080: 178-206, 2006.
47. Maltsev VA and Lakatta EG: Dynamic interactions of an intracellular Ca2+ clock and membrane ion channel clock underlie robust initiation and regulation of cardiac pacemaker function. Cardiovasc Res 77: 274-284, 2008.
48. Lakatta EG, Maltsev VA and Vinogradova TM: A coupled SYSTEM of intracellular Ca2+ clocks and surface membrane voltage clocks controls the timekeeping mechanism of the heart's pacemaker. Circ Res 106: 659-673, 2010.
49. Espinoza-Lewis RA, Liu H, Sun C, Chen C, Jiao K and Chen Y: Ectopic expression of Nkx2.5 suppresses the formation of the sinoatrial node in mice. Dev Biol 356: 359-369, 2011.